Hindawi Publishing Corporation
Advances in Civil Engineering
Volume 2012, Article ID 267584, 10 pages
doi:10.1155/2012/267584

Research Article

Pounding Effects in Simply Supported Bridges Accounting for Spatial Variability of Ground Motion: A Case Study

G. Tecchio, M. Grendene, and C. Modena

Department of Structural and Transportation Engineering, University of Padova, Via Marzolo 9, 35131 Padova, Italy

Correspondence should be addressed to G. Tecchio, tecchio@dic.unipd.it

Received 2 January 2012; Accepted 24 March 2012

Academic Editor: Sami W. Tabsh

This study carries out a parametrical analysis of the seismic response to asynchronous earthquake ground motion of a long multispan rc bridge, the Fener bridge, located on a high seismicity area in the north-east of Italy. A parametrical analysis has been performed investigating the influence of the seismic input correlation level on the structural response: a series of nonlinear time history analyses have been executed, in which the variation of the frequency content in the accelerograms at the pier bases has been described by considering the power spectral density function (PSD) and the coherency function (CF). In order to include the effects due to the main nonlinear behaviours of the bridge components, a 3D finite element model has been developed, in which the pounding of decks at cap-beams, the friction of beams at bearings, and the hysteretic behaviour of piers have been accounted for. The sensitivity analysis has shown that the asynchronism of ground motion greatly influences pounding forces and deck-pier differential displacements, and these effects have to be accurately taken into account for the design and the vulnerability assessment of long multispan simply supported bridges.

1. Introduction

Earthquake ground motion is usually assumed as a spatially uniform dynamic input in seismic analysis; this assumption is correct for structures standing on a reasonably restricted area, in which the soil characteristics are presumed to be homogeneous and the seismic wave propagating velocity can be neglected, but becomes inadequate for spatial structures standing on large sites such as extended foundations or dams, and long-estending structures such as bridges, viaducts, tunnels, and pipelines. In these cases the spatial variability of ground motion should be considered to avoid gross evaluation errors or at least underestimation of the dynamic response, since the phenomenon affects the response considerably and, hence, the level of protection of these structures (Lupoi et al. [1]). In particular for long multispan simply supported bridges, a spatial variation in the input acting at supports (pier and abutment foundations) should be considered since it can induce pounding effects and deck unseating. It has been observed during the recent major seismic events that this kind of bridge structure very often experiences pounding phenomena between adjacent structural segments (between neighbouring decks or cap-beams and decks, with a component of impact force transferred to the piers), which can amplify differential movements between adjacent spans and determine cracks or brittle fractures at beam endings. These amplified differential displacements can induce pull-off and drop collapses of spans when the displacement capacity of the bearing devices is exceeded or the seating length of girders is not sufficient for them to rest on their supports during strong ground motions.

For this type of bridges are required quite complex numerical models to represent with acceptable approximation the global structural response taking into account the incoherency of the seismic excitation at the supports, the impact phenomena between neighbouring structural segments, and the nonlinear behaviour of the substructural components (piers and decks).

In the present study, the acceleration and displacement time histories at the several prescribed locations on the ground surface corresponding to the bridge supports, are generated using the spectral representation method [2–4]. In order to generate the stochastic field, three basic components are required: (i) power spectral density (PSD) which gives the frequency content of the random process, (ii) coherency function (CF) which gives an analytical representation of

spatial variation of the ground motion in the frequency domain, and (iii) shape function (SF) for determining a nonstationary random process in the time domain. Some expressions have been proposed for the target spectral density (i.e., the Clough-Penzien form [5], and the expressions given by seismic codes [6]), for the coherency function [7–10] for the shape function [9]. The generated time histories are compatible with prescribed response spectra and duration of strong ground motions for the considered seismic area and reflect the wave passage and loss of coherence effects.

As regards evaluation of the pounding effects, it has to be said that the interest of researchers is quite recent; the problem was first investigated by [11] who studied the pounding phenomenon between two adjacent buildings, modelling the collision through impact elements which connected simple single-degree of freedom structures. In 1992 the same problem was examined also by [12]; in 1998 the study made by [11] was taken up again and applied to bridge structures in [13]. Further investigations were developed in [14] on the numerical simulation of the pounding process with the aim of calibrating the impact element between neighbouring structures by comparing the numerical results with the exact solution based on the wave propagation theory. In recent years more complex finite elements models have been developed: a numerical 3D simulation applied to a multispan simply supported bridge is described in [15].

From the aforementioned studies interesting conclusions can be drown for an improved modelling of the pounding effect:

(1) pounding between adjacent segments can be described with fair accuracy through an impact element characterised by stiffness and damping (which accounts for energy dissipation);

(2) it has been noted in [13] that there is no need of modelling the entire structure for long bridges in order to assess the middle span response with fair accuracy; it is enough to study the seven central spans since there are no relevant differences in the numerical results between a model with an infinite number of span and a seven-span model;

(3) in the finite element model the stiffness k_1 of the impact element should be calibrated considering the number n of finite elements which compose the deck ([14]);

(4) it is important to define opportunely the time step used for the integration in the time-domain to avoid that colliding adjacent segments of neighbouring decks may behave like rigid bodies, since they influence the dynamic response with their axial deformation.

In the present study state-of-the-art models have been used to simulate the asynchronous ground motion as a multisupport seismic excitation and describe the pounding effects, as described in Section 2.

Figure 1: Fener bridge: (a) lateral view of the bridge on the Piave river.

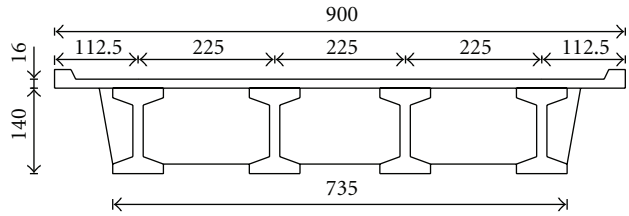

Figure 2: Typical transverse section of the superstructure.

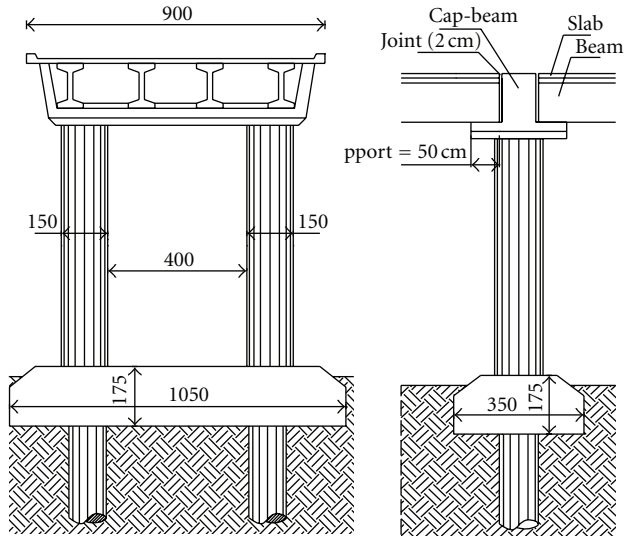

Figure 3: Pier elevation and longitudinal section.

2. Seismic Response Accounting for Spatial Variability of Ground Motion: A Sensitivity Analysis

2.1. The Fener Bridge. This study carries out a parametrical analysis of the seismic response to asynchronous earthquake ground motion of a long multispan rc bridge, the Fener bridge (see Figures 1, 2, 3 and 4), located in the Veneto region, in the Treviso province.

It represents an important overcrossing of the Piave river for the region road network. It was built in the mid nineteen seventies, and it consists of 24 regular spans having the same length of 24.75 m, except for the lateral spans near abutments, which are shorter (in particular at one end there

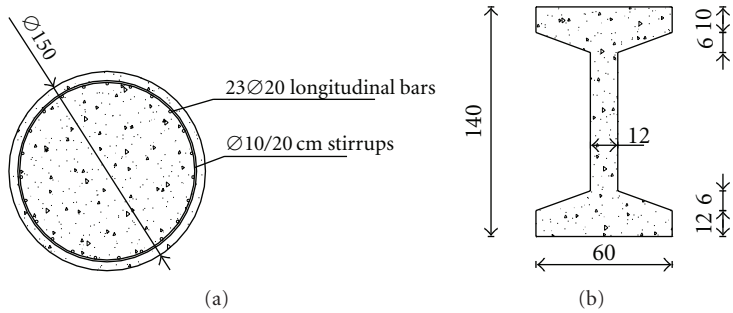

Figure 4: Cross sections of (a) typical column with reinforcement and (b) typical longitudinal precast concrete beam.

are two spans with reduced lengths of 18 m and 17.5 m, respectively, whilst at the other end only the last span has a slightly shorter lenght of 23.75 m). The overall structure is about 579 m long.

The deck lodging two lanes has an overall width of 9 metres; the deck structure is made up by four I-shaped precast beams with a constant height of 1.4 m and by a 16 cm high rc slab. The transverse distribution of traffic loads is obtained through 3 orthogonal rc girders positioned in the middle and at both ends of each span. Piers have a portal-shaped structure with circular rc columns, whose height varies gradually along the plan from a minimum of 5 to 8 m roughly, since the deck slope in the longitudinal direction is about 2%, while the extrados levels of plinths at the base remain constant. Piers raise on deep foundations as illustrated in Figure 3.

The pier section is shown in Figure 4(a): reinforcement for each of the two columns is provided by 23 longitudinal bars of 20 mm diameter and transverse stirrups of 10 mm diameter (pitch = 20 cm).

The materials used for piers can be classified as follows:

(i) concrete: grade C25/30;

(ii) reinforcing steel: smooth bars, characteristic yield stress f_{yk} = 315 MPa.

According to the national seismic zonation map, Fener bridge is located in an area characterised by PGA = 0.25 g, on a soil of medium stiffness (type B soil, according to the national zonation map [16]).

2.2. FE Model of the Multisupported Structure. In the numerical model of the bridge elements with linear and nonlinear behaviour have been adopted in order to represent effectively the global structural response: main beams, cap-beams, and transverse girders have been modelled with linear beam elements, the rc slab has been modelled with plate elements, whilst a nonlinear behaviour has been adopted for columns to simulate their hysteretic behaviour (using the Takeda-model [17] see Figure 5), for gap elements simulating impact between adjacent structural segments, and for frictional connections between longitudinal beams and cap-beams.

For the pier-element it has been necessary to assign in input a nonlinear force-displacement law, which has been obtained through a push-over analysis both in the longitudinal direction, where the column has a cantilever deflection, and in the transverse direction where the piers behaviour is that of a portal frame. A lumped plasticity element has been employed for modelling the piers; the derived force-displacement curves are plotted below (see Figures 7 and 8).

Girders sit on cap-beams without any bearing devices therefore restraint of superstructure segments from longitudinal displacement is given only by friction; the force-displacement law for frictional bearings is assumed as an idealized rigid-plastic behaviour, with a friction coefficient taken as $\mu = 0.60$ in the analysis (see Figure 6). In the transverse direction a rigid restraint between deck and cap beam is assumed: the cap-beam lateral sides, being in direct contact with beams and acting as shear keys, do not allow any differential displacement.

Pier-deck pounding has been modelled through nonlinear gap elements which react only under compression, after the initial gap closure corresponding to the joint width (2 cm).

The gap element stiffness k_1 has been determined normalising to 1 parameter γ in the following expression [14]:

$$\gamma = \frac{k_1 L}{nEA}, \tag{1}$$

where A is the deck cross section, E its elastic modulus, L the span length, and n the number of finite elements into which the span length has been divided, taken as $n = 10$ in this study. In particular for the impact element a damping equivalent to energy dissipation has not been considered and a perfectly elastic collision has been modelled since impact energy dissipation does not influence the global structure response significantly [13].

As to external restraints, they have been considered fixed both in translation and rotation, because foundations are plinths on piles and in a first approximation the soil-structure interaction can be neglected. The superstructure segments not considered in the model (which represent a boundary condition to it) have been substituted with gap elements as illustrated in [13].

The FE model of the bridge and the related nonlinear dynamic analyses have been performed using *CSI SAP2000 release 9* software [18]. The model represents only the 7 central spans of the bridge (see Figure 9), with adequate

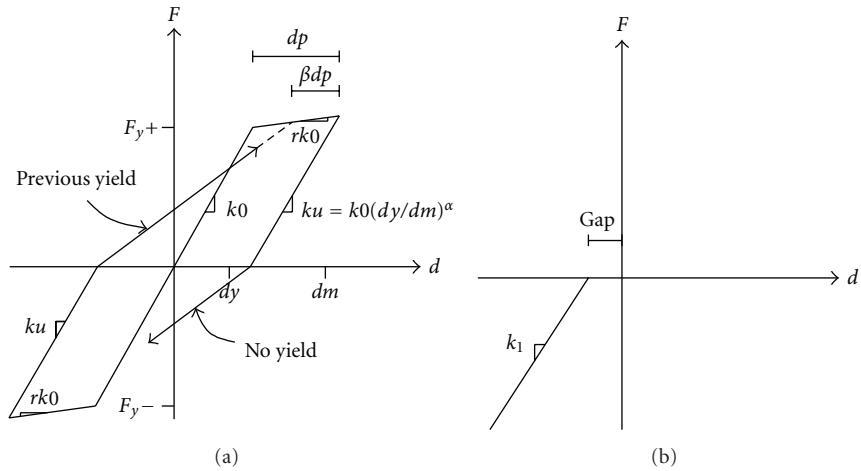

Figure 5: Models for (a) hysteretic behaviour of piers (Takeda model) and (b) gap element between adjacent structural segments.

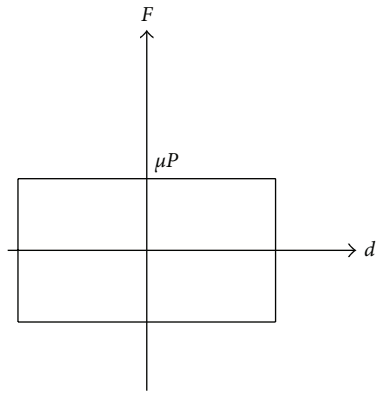

Figure 6: Connection between girder and cap-beam (frictional behaviour).

boundary conditions, instead of all the 24 spans; this has allowed to reduce substantially the computational effort due to the nonlinear effects included, without influencing the numerical accuracy of results because, as reported in [13], the seismic response of the central span in a model with a number of spans not less than five is a good approximation of the response obtained modelling the complete structure.

2.3. Charactherisation of Spatial Variability. In the present study, the acceleration and displacement time histories at several prescribed locations on the ground surface corresponding to the bridge supports are generated using the spectral representation method. A uniform soil type is considered. As mentioned before, in order to generate the stochastic field, three basic components are required: (i) power spectral density function, (ii) coherency function, and (iii) shape function.

2.3.1. Power Spectral Density Function. Different analytical models for PSD are advanced by some authors; in this study the expressions given in EC8 [6] have been used, which are approximate relations for power spectra corresponding to the site-dependent response spectrum proposed in the code. The expressions are derived as follows:

$$\begin{aligned} S_a &= 0.2\xi' A^2 T^{1.4} \quad \text{for } T < T_B, \\ S_a &= 6\xi' V^2 T^{-0.74} \quad \text{for } T_B < T < T_c, \\ S_a &= 300\xi' D^2 T^{-3.1} \quad \text{for } T > T_c, \end{aligned} \tag{2}$$

where S_a is the acceleration power spectrum, ξ' is the value of the damping ratio, A, V, and D are the values of spectral acceleration, velocity and displacement, and T_B and T_C are the response spectrum parameters.

2.3.2. Coherency Function. Assuming that the seismic wave field can be completely described by a single plane vawe, its spatial variation can be quantified by means of the coherency function, which expresses the dependence in the frequency domain between the PSD of time histories ground motions occuring at two different stations k and l (with relative distance given by d_{kl}) [15]. It is generally defined as follows:

$$\gamma_{kl}(\omega) = \begin{cases} \dfrac{S_{kl}(\omega)}{\sqrt{S_{kk}(\omega) \cdot S_{ll}(\omega)}} & \text{for } S_{kk} \neq S_{ll}, \\ 0 & \text{for } S_{kk} \cdot S_{ll} = 0, \end{cases} \tag{3}$$

where ω is the circular frequency, $S_{kk}(\omega)$ and $S_{ll}(\omega)$ denote the autopower spectral density of the time histories at the stations k and l and $S_{kl}(\omega)$ is the cross-spectral density function of the considered pair of processes.

In general $\gamma_{kl}(\omega)$ is complex valued; its bounded modulus $0 \leq |\gamma_{kl}(\omega)| \leq 1$ measures the linear statistical dependence between the two time-histories: in particular $\gamma_{kl} = 1$ represents perfect correlation between the two motions, whereas $\gamma_{kl} = 0$ denotes complete lack of linear dependence, which means totally uncorrelated signals.

There are several models available in literature for the coherency function; in the present study the formulation

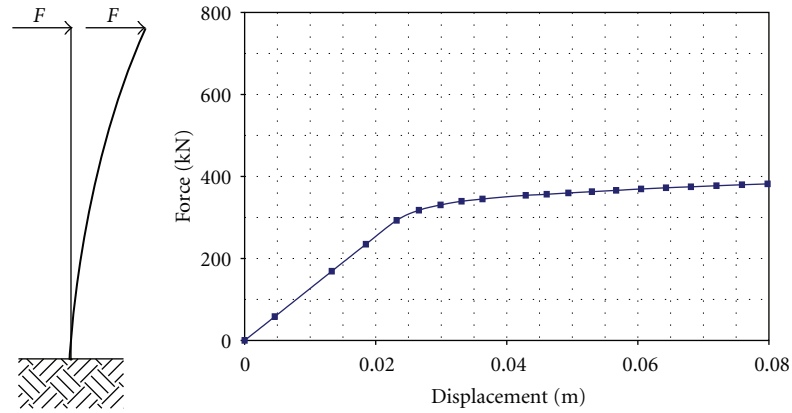

Figure 7: Piers behaviour in the longitudinal direction: (a) deflection shape; (b) force-displacement curve.

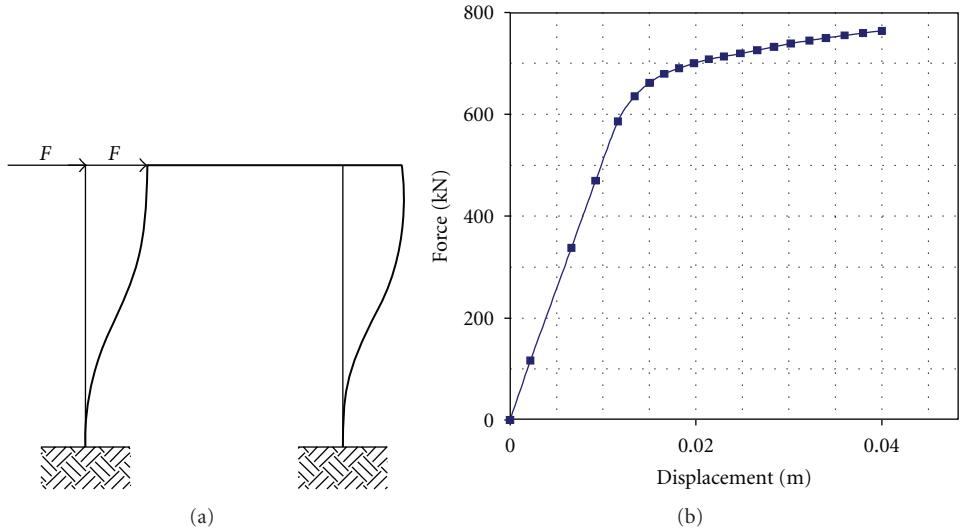

Figure 8: (a) Piers behaviour in the transverse direction: deflection shape; (b) force-displacement curve.

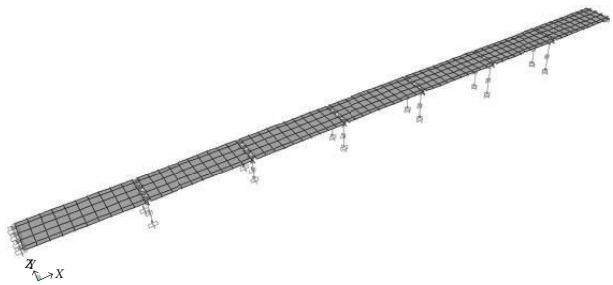

Figure 9: Three-dimensional FE model of the seven central spans.

given in [10] has been adopted (see Figure 10), and its general expression is

$$\gamma_{kl}(d_{kl},\omega) = \exp\left\{-\left(\frac{\alpha\cdot\omega\cdot d_{kl}}{v_s}\right)^2\right\}\cdot\exp\left\{i\frac{\omega\cdot d_{kl}}{v_{\text{app}}}\right\}, \quad (4)$$

where the first term represents the geometrical incoherence, which arises from the scattering of waves in the heterogeneous soil medium, while the second term accounts for the velocity of seismic waves and the difference in the times of arrival at different stations (vawe-passage effect). The parameters describing these phenomena are, respectively (v_s/α), in which v_s is the shear wave velocity in the medium, α a measure of loss of the coherency rate with distance and frequency, v_{app}, is the value of the apparent horizontal velocity of the surface wave. The relative distance between the two different stations k and l is given by the span length d_{kl}, while ω is the circular frequency. Both parameters (v_s/α) and v_{app} usually vary in the range $[300\,\text{m/s},\infty[$; if $(v_s/\alpha) \to \infty$ and $v_{\text{app}} \to \infty$, the modulus of coherency function tends to be 1: the two signals are then totally correlated (identical and in-phase ground motions).

2.3.3. Shape Function. The shape function of the oscillatory process is defined in a general exponential form as suggested in [15]; it is the normalised envelope function of the time history and is governed by the parameters t_1 and t_2 which define the ramp duration and the decay starting time; $t_{\max}$

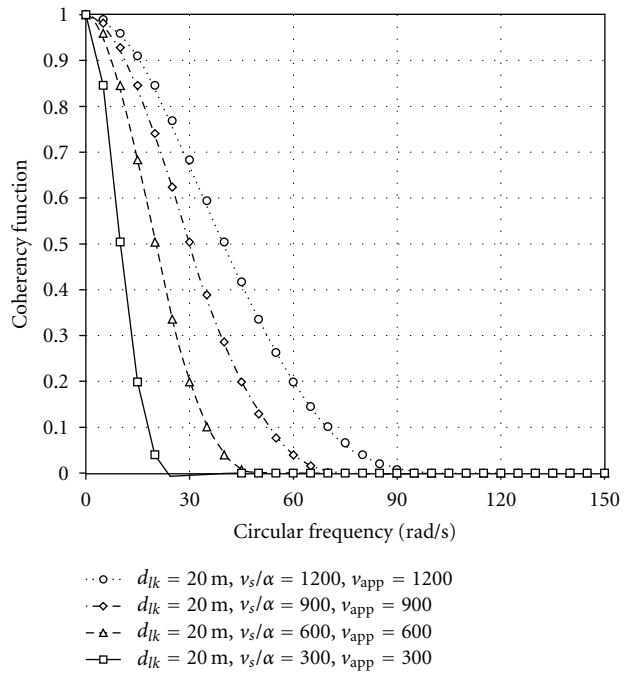

Figure 10: Coherency function modulus obtained for different correlation levels corresponding to a set of 4 values of parameters v_s/α e v_{app} (formulation by Luco and Wong).

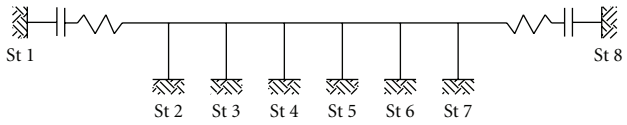

Figure 11: Ray of the 8 stations implemented in the FE model of the structure.

is the time history duration and $\nu = 0.2$ is the ratio of the amplitude envelope. The analytical formulation is as follows:

$$\xi(t) = \begin{cases} (t/t_1)^{\eta}, & t \le t_1, \\ 1, & t_1 \le t \le t_2, \\ \exp\left\{\dfrac{t - t_2}{t_{\max} - t_2} \ln \nu\right\}, & t_2 \le t \le t_{\max}. \end{cases} \quad (5)$$

The parameters values in this work are taken as follows: $t_1 = 6$ sec, $t_2 = 16$ sec, $t_{\max} = 40$ sec, $\eta = 2.0$, and $\nu = 0.02$.

2.4. Generation of Compatible Time History Sets. In this study the formulation proposed in [6] for target spectral density function has been used to generate time history sets compatible with the response spectrum given by the code for a soil of medium stiffness with PGA = 0,25 g. The accelerograms, based on the coherency function previously described, have been generated trough the implementation of opportune alghoritms [2]; the nonstationarity has been impressed to the stationary simulated motions by means of the shape function. In order to use the generated sets of response spectrum and coherency compatible time histories as multisupport seismic inputs at the stations numbered from 1 to 8 (see Figure 11), the acceleration time histories have been doubly integrated to obtain the corresponding displacement time histories [15].

Different patterns of coherency have been selected in the parametric study, in order to represent the intermediate levels between the full correlation and the total uncorrelation of the time histories: 16 combinations of parameters v_s/α and v_{app} varying in the interval 300–1200 m/s have been considered (see Table 1), and for each combination five sets of generated time histories associated with a linear array of 8 stations (corresponding to locations of piers in the 7 central modelled spans of the bridge) have been applied, for a total of 80 sets examined.

A superimposition of the displacement time-histories generated in the simulation is reported as an example in Figure 12; the two extreme cases of strongly correlated ground motions (v_s/α = 1200 m/s, v_{app} = 1200 m/s) and weakly correlated motions at supports (v_s/α = 300 m/s, v_{app} = 300 m/s) are presented for the 8 stations considered in the analysis.

2.5. Analysis in the Time Domain. In order to determine the nonlinear response of the structure to a large set of earthquake ground excitations, it is necessary to use an efficient and not much time-consuming time-integration algorithm; in the present study the mode superimposition procedure based on load-dependent Ritz vectors [19] has been employed instead of direct integration methods in the time domain to reduce the computational effort and maintain an accurate solution. Further, the duration of the time step used for the integration has been limited by the follows condition:

$$\Delta t < T_1, \quad (6)$$

where T_1 is the expected impact duration. Thus it has been possible to capture in the model the effect that colliding adjacent segments of neighbouring decks produce by behaving not like rigid bodies, but influencing the dynamic response with their axial deformation [20]. The impact duration is calculated as follows:

$$T_1 = \frac{2L}{C_0}, \quad (7)$$

where L is the span length of the deck subjected to the pounding effect and C_0 is the propagation velocity of the impact wave travelling in a continuous medium, defined as follows:

$$C_0 = \sqrt{\frac{E}{\rho}}, \quad (8)$$

with E representing the elastic modulus of the superstucture and ρ its density

The values calculated for T_1 and the corresponding Δt adopted in this study are listed in Table 2.

It should be noticed that in fact a superstructure segment does not hit the neighbouring deck directly, due to the

Table 1: Combinations of v_s/α and v_{app} values considered in the parametric study.

Vawe-passage effect	Geometrical incoherence v_s/α (m/s)			
v_{app} (m/s)	300	600	900	1200
300	x	x	X	x
600	x	x	X	x
900	x	x	X	x
1200	x	x	X	x

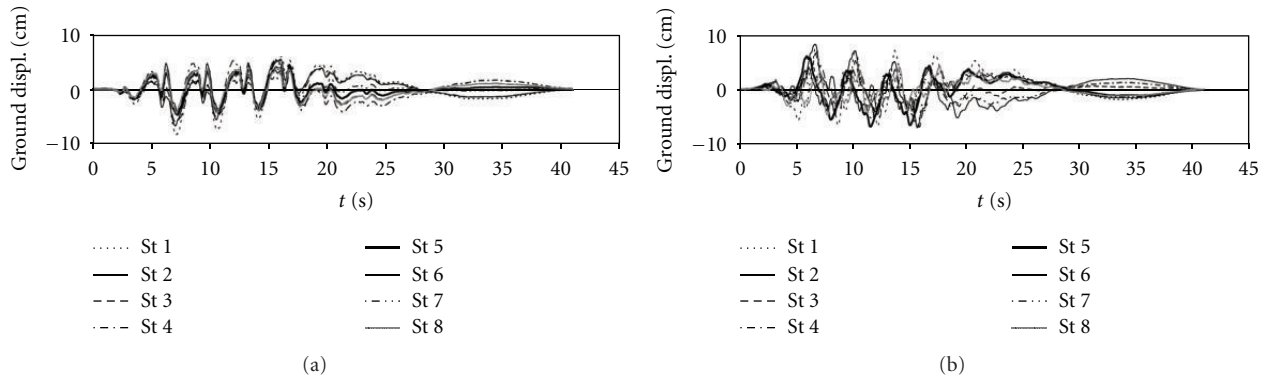

Figure 12: Displacement time histories for stations 1 to 8: (a) highly correlated time-histories (set 1/5 v_s/α = 1200 m/s.

Table 2: Integration time step adopted Δt.

Elastic modulus E (MPa)	24821
Density ρ (Kg/m^3)	2500
Deck span lenght L (m)	24.75
Impact duration T_1 (s)	0.016
Integration time step Δt (s)	0.01
$\Delta t/T_1$	0.625

presence of the cap beam, but this element has been assumed as transmitting the impact rigidly and not influencing the wave propagation.

3. Results of the Numerical Analyses

A sensitivity analysis of the structure dynamic behaviour due to different spatially varying ground motion sets has been carried out, evaluating the influence of the seismic input correlation on the structural response, in terms of the following:

(i) differential displacement between piers and deck segments;

(ii) pounding forces between cap-beams and decks;

(iii) effects on piers: shear forces at the bases and maximum displacements at the tops.

The response analysis focuses on the central span of the FE model, in order to provide results unaffected by the boundary coditions; as previously said, for each prefixed level of ground motion correlation (16 in total, each one determined by a couple of the parameters v_s/α and v_{app}) 5 nonlinear dynamic analyses have been performed, using compatible time history sets. The mean value of the five results has been adopted.

3.1. Differential Displacements. Differential displacements between piers and decks are represented in Figure 13: it can be observed that in all cases the calculated values are relatively small and remain under the threshold of 5 cm; the maximum differential displacement (d_d = 4.4 cm) is obtained, as expected, for the extreme case of maximum coherency loss (v_s/α = 300 m/s, v_{app} = 300 m/s).

The limited amplitude of differential displacements prevents pull-off-and-drop collapse of deck segments and can be explained considering that joint gaps at span ends are small (2 cm) and do not allow the development of high inertia forces at the deck level; consequently the displacements cannot be considerably amplified. These results are in accordance with the observations reported in [20].

3.2. Pounding Forces. Impact forces between cap beams and decks are highly influenced by the correlation level of ground motions at the structural supports: as Figure 14(a) shows, there is a trend in pounding forces, which rapidly increase with the loss of coherency of seismic inputs: the magnitude of impact force F_I, obtained in the extreme case of weakly correlated time histories (v_s/α = 300 m/s, v_{app} = 300 m/s), assumes a value 3 times larger (F_I = 1293 kN) than that derived by analysis with uniform inputs, F_I = 428 kN (represented by the case v_s/α = 1200 m/s, v_{app} = 1200 m/s). Consequently, even though in the case of uniform seismic excitation no damage should occur to the cap beams and decks, with weakly correlated input time histories, the pounding effects could determine considerable damage to the local area of bridge decks.

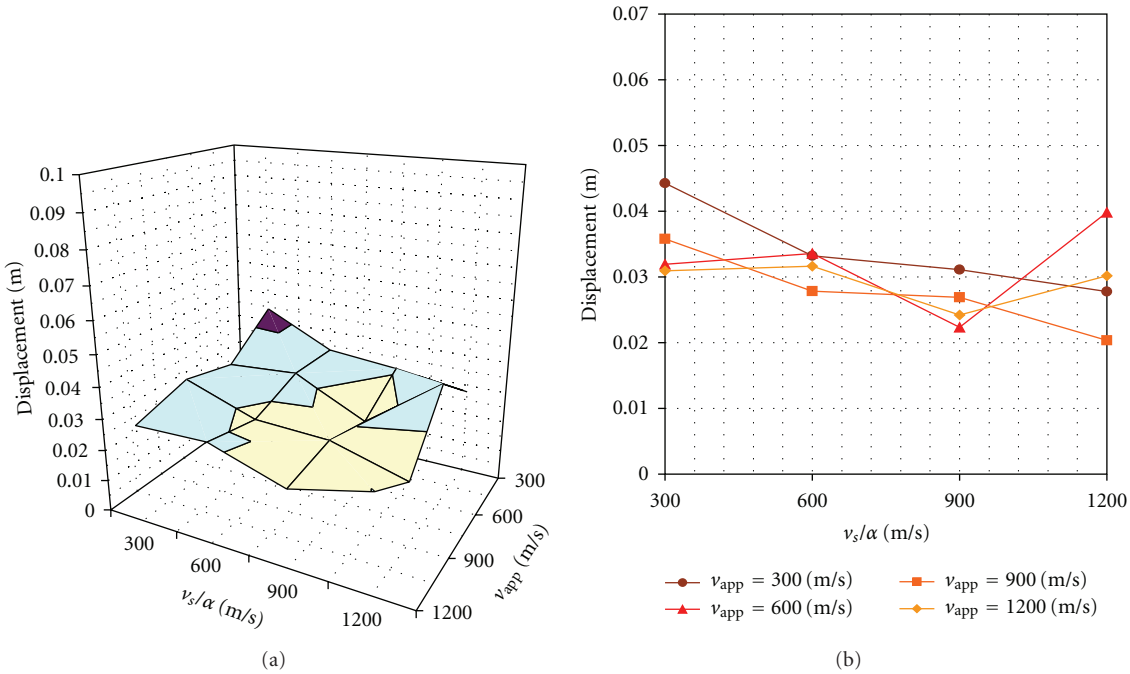

FIGURE 13: Pier-deck differential displacement varying with seismic input correlation level (represented by parameters v_s/α and v_{app}): (a) 3D view and (b) 2D view.

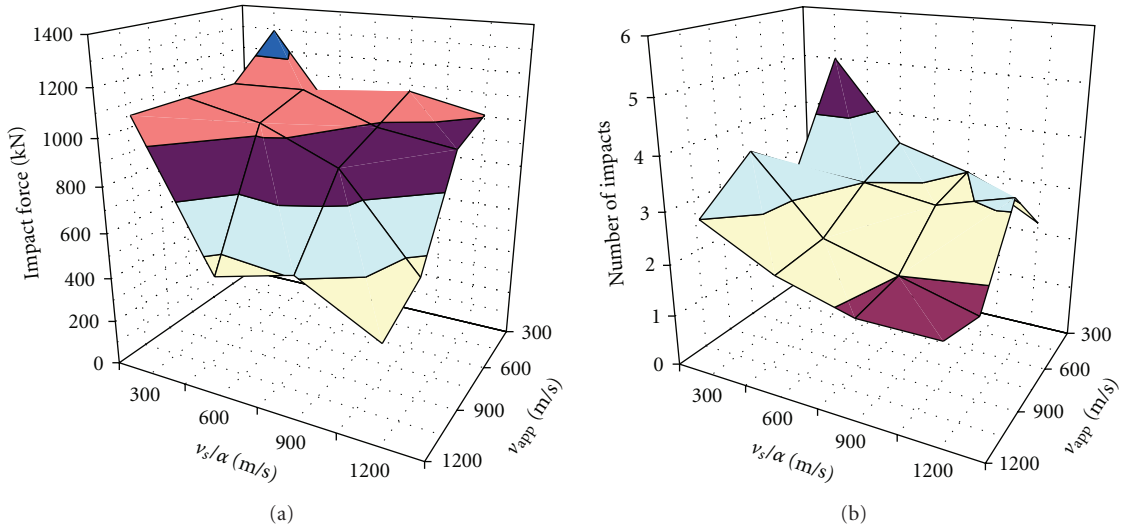

FIGURE 14: (a) Pounding forces varying with correlation level of input ground motions; (b) Total number of registered impacts (mean value).

Registered impacts follow a similar tendency (see Figure 14(b)): the numerical results show that collisions occur more frequently as the correlation level of time history inputs decreases. However in all cases, the total number of impacts (mean value of the 5 non linear dynamic analysis performed) is found to be relatively small (less than 5).

3.3. Effects on Piers. As regards the effects on piers in the longitudinal direction, they are represented in Figure 15 in terms of shear forces and displacements (maximum values at the top of the pier) obtained as functions of the correlation level between the time histories. It can be observed that the maximum value of shear force $V = 346$ kN is obtained in the case of highly correlated time histories, and the minimum $V = 274$ kN is derived using inputs with the weakest correlation ($v_s/\alpha = 300$ m/s, $v_{app} = 300$ m/s). Similarly it can be said that there is a general trend for displacements at the pier top (see Figure 15(b)) that become larger as the correlation increases, with the maximum value $D = 3{,}7$ cm calculated in the case of the highest correlation level of input ground motions.

These effects can be explained considering that when ground excitations are weakly correlated or uncorrelated, the movement of deck segments can be in opposite direction

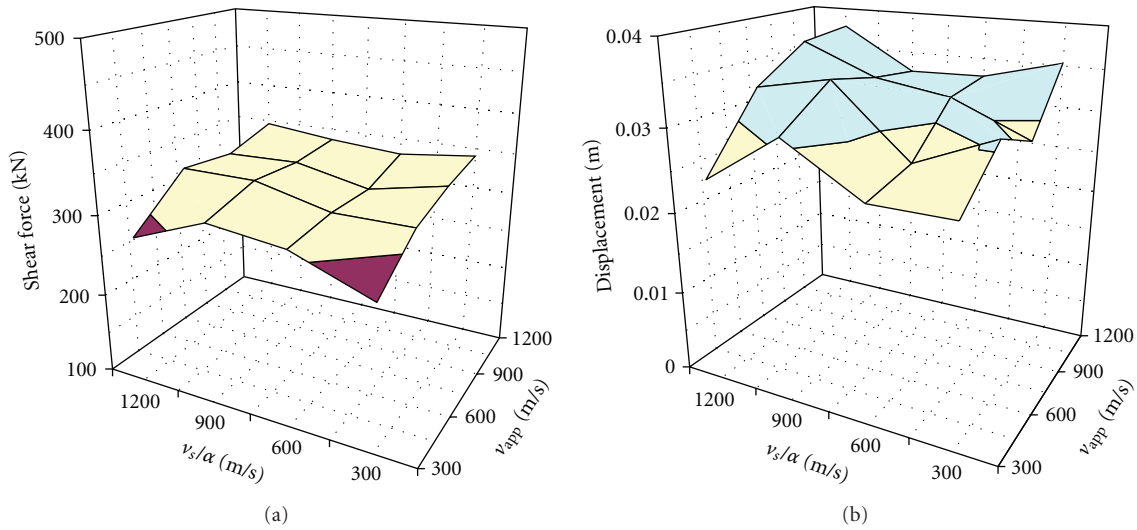

Figure 15: Longitudinal direction: (a) shear forces at the pier base: maximum values obtained for each correlation level of input ground motions; (b) maxima values of displacement at pier top.

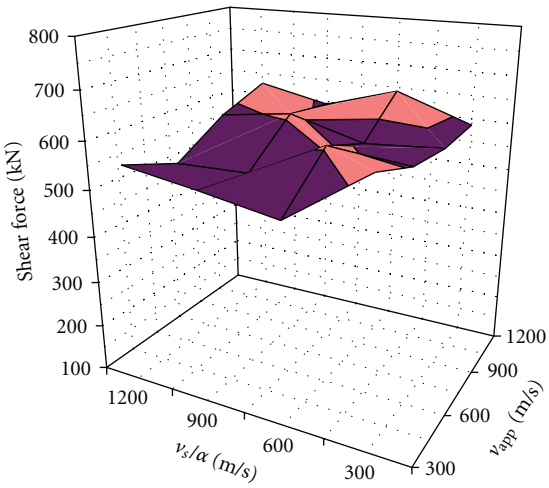

Figure 16: Transverse direction: maximum shear forces.

due to out-of-phase vibrations, and this fact determines collisions that reduce displacements at the top of the pier (and consequently the shear and bending moment at the base induced by the deformation of the pier itself). When the ground excitation is highly correlated, the responses of the bridge spans are in phase, the inertial forces at the pier tops are maximised, and in consequence displacements at the top and shear forces increase.

Regarding the response in the transverse direction, it should be noted that structural behaviour is not clearly affected by seismic input correlation (see Figure 16); one can observe that there is a slight tendency for shear forces at the pier base to increase with higher correlation levels, but the values are weakly affected by impacts between deck segments. This is consistent with the results presented in [19].

4. Conclusions

A parametrical analysis has been performed with the aim of investigating the influence of the seismic input correlation level on the structural response of a long multispan girder bridge. A series of nonlinear time history analyses have been performed, in which the main nonlinear behaviours of the bridge components, have been included: (i) the pounding of decks at cap-beams, (ii) the friction of beams at bearings, and (iii) the hysteretic behaviour of piers. The following conclusions can be drawn:

(i) differential displacements between decks and pier-tops are affected by input correlation level but remain within a limited range (under the threshold of 5 cm) with the maximum value obtained for the extreme case of maximum coherency loss. The fact that they are relatively small prevents decks from unseating and can be explained by the limited width of the bridge joints;

(ii) asynchronous ground motion influences greatly the pounding forces between decks and pier-tops, which can assume values 3 times larger than those calculated by an analysis with uniform input (represented by the case with the highest correlation level between the time-histories). The amplified pounding effects might determine considerable damage to the local area of bridge decks;

(iii) as regards the effects on piers, it can be observed that in the longitudinal direction there is a general trend for displacements and shear forces, which increase with higher correlation levels of input ground motions. In the transverse direction the seismic response is not clearly influenced by the correlation level of ground excitations.

The results highlight that the spatial variation properties of the earthquake ground motion can significantly change the structural response especially in terms of pounding forces and deck unseating, and consequently these effects have to be taken into account for the design or the vulnerability assessment of long multispan simply supported bridges.

References

[1] A. Lupoi, P. Franchin, P. E. Pinto, and G. Monti, "Seismic design of bridges accounting for spatial variability of ground motion," *Earthquake Engineering and Structural Dynamics*, vol. 34, no. 4-5, pp. 327–348, 2005.

[2] G. Deodatis, "Non-stationary stochastic vector processes: seismic ground motion applications," *Probabilistic Engineering Mechanics*, vol. 11, no. 3, pp. 149–167, 1996.

[3] M. Shinozuka and G. I. Schueller, "Stocastic fields and their digital simulation," in *Stochastic Methods in Structural Dynamics*, G. I. Schueller and M. Shinozuka, Eds., pp. 93–133, Martinus Nijhoff, Dordrecht, The Netherdands, 1987.

[4] M. Shinozuka and G. Deodatis, "Simulation of multi-dimensional Gaussian stochastic fields by spectral representation," *Applied Mechanics Reviews*, vol. 44, no. 4, pp. 191–204, 1991.

[5] R. W. Clough and J. Penzien, *Dynamics of Structures*, McGraw Hill, New York, NY, USA, 1993, International Edition.

[6] UNI ENV 1998-2, "Eurocode 8—design provisions for earthquake resistance of structures—part 2," Bridges, 1998.

[7] A. Der Kiureghian, "A coherency model for spatially varying ground motions," *Earthquake Engineering and Structural Dynamics*, vol. 25, no. 1, pp. 99–111, 1996.

[8] H. Hao, C. S. Oliveira, and J. Penzien, "Multiple-station ground motion processing and simulation based on smart-1 array data," *Nuclear Engineering and Design*, vol. 111, no. 3, pp. 293–310, 1989.

[9] R. S. Harichandran and E. H. Vanmarcke, "Stochastic variation of earthquake ground motion in space and time," *ASCE Journal of Engineering Mechanics*, vol. 112, no. 2, pp. 154–174, 1986.

[10] J. E. Luco and H. L. Wong, "Response of a rigid foundation to a spatially random round motion," *Earthquake Engineering and Structural Dynamics*, vol. 14, no. 6, pp. 891–908, 1986.

[11] S. A. Anagnostopoulos, "Pounding of buildings in series during earthquakes," *Earthquake Engineering and Structural Dynamics*, vol. 16, no. 3, pp. 443–456, 1988.

[12] B. F. Maison and K. Kasai, "Dynamics of pounding when two buildings collide," *Earthquake Engineering and Structural Dynamics*, vol. 21, no. 9, pp. 771–786, 1992.

[13] R. Jankowski, K. Wilde, and Y. Fujino, "Pounding of superstructure segments in isolated elevated bridge during earthquakes," *Earthquake Engineering and Structural Dynamics*, vol. 27, no. 5, pp. 487–502, 1998.

[14] K. Kawashima and Watanabe G., "Numerical simulation of pounding of bridge decks," in *Proceedings of the 13th World Conference on Earthquake Engineering Vancouver*, British Columbia, Canada, August 2004, Paper no.884.

[15] G. Zanardo, H. Hao, and C. Modena, "Seismic response of multi-span simply supported bridges to a spatially varying earthquake ground motion," *Earthquake Engineering and Structural Dynamics*, vol. 31, no. 6, pp. 1325–1345, 2002.

[16] Ordinance of the Presidency of the Council of Ministers 3431, "Initial elements on the general criteria for classifying national seismic zones and technical standards for construction," *Official Gazette of the Italian Republic, 2003*.

[17] T. Takeda, A. M. Sozen, and N. N. Nielsen, "Reinforced concrete response to simulate earthquakes," *ASCE Journal of Structural Engineering Division*, vol. 96, no. 12, pp. 2257–2273, 1970.

[18] Computers & Structures Inc., "*CSI SAP2000 release 9*," Berkeley Calif, USA, 2004.

[19] E. L. Wilson, M. W. Yuan, and J. M. Dickens, "Dynamic Analysis by direct superposition of Ritz vectors," *Earthquake Engineering and Structural Dynamics*, vol. 10, no. 6, pp. 813–821, 1982.

[20] R. Jankowski, K. Wilde, and Y. Fujino, "Reduction of effects in elevated bridges during earthquakes," *Earthquake Engineering & Strucutral Dynamics*, vol. 29, pp. 195–212, 2000.